Electronic Supplementary Material (ESI) for Physical Chemistry Chemical Physics.

Supporting Information for

Photochemically triggered cheletropic formation of cyclopropenone (c-C_3H_2O) from carbon monoxide and electronically excited acetylene

Jia Wang[1,2], N. Fabian Kleimeier[1,2], Rebecca N. Johnson,[3] Samer Gozem[3]*, Matthew J. Abplanalp[1,2], Andrew M. Turner[1,2], Joshua H. Marks[1,2], Ralf I. Kaiser[1,2]*

[1] *Department of Chemistry, University of Hawaii at Manoa, Honolulu, HI 96822, USA*

[2] *W. M. Keck Research Laboratory in Astrochemistry, University of Hawaii at Manoa, Honolulu, HI 96822, USA*

[3] *Department of Chemistry, Georgia State University, Atlanta, GA 30302, USA*

*Corresponding Authors: sgozem@gsu.edu, ralfk@hawaii.edu

Experimental details

The silver mirror serves as a substrate and can be rotated in its horizontal plane by using a doubly differentially pumped rotational feedthrough (Thermionics Vacuum Products, RNN-600/FA/MCO) and translated vertically by a movable UHV compatible bellow (McAllister, BLT106).[1] By combining a zeolite absorber cartridge (Chromatography Research Systems, Model 300) and a dry ice-ethanol slush bath, the trace amounts of the stabilizer, acetone from the acetylene-d_2 gas were removed prior to the mixing process with the $C^{18}O$ gas.[1] The deposition processes were monitored by laser interferometry with a helium-neon (HeNe) laser (CVI Melles-Griot; 25-LHP-230, 632.8 nm). During deposition, the interference fringes were recorded to determine the thickness of the ice.[2] To quantify the ratio of the ice constituents, the IR spectra of pure $C^{18}O$ and C_2D_2 ices of known thicknesses were measured. An ice ratio of (1.1 ± 0.1) :(1.0 ± 0.4) for $C^{18}O$ – C_2D_2 was determined based on the IR spectrum of the mixed ice. The absorption coefficients of infrared peaks at 1077 cm^{-1} ($\nu_4+\nu_5$, C_2D_2), 2929 cm^{-1} ($\nu_3+\nu_4$, C_2D_2), 2088 cm^{-1} (ν_1, $C^{18}O$), 3294 cm^{-1} ($\nu_1+\nu_5$, C_2D_2), 4150 cm^{-1} ($2\nu_1$, $C^{18}O$) are experimentally determined as 3.5×10^{-19} cm molecules^{-1}, 1.3×10^{-18} cm molecules^{-1}, 4.9×10^{-20} cm molecules^{-1}, 2.5×10^{-19} cm molecules^{-1}, and 6.6×10^{-20} cm molecules^{-1}, respectively. A dye laser used for irradiation was pumped by the second (for 288 nm) or third (for 249 nm and 222 nm) harmonic of Nd:YAG laser (Spectra-Physics, Quanta-Ray Pro-270) operating at 30 Hz. The dyes used for generating 222 nm, 249 nm and 288 nm were Coumarin 450, Coumarin 503, Pyrromethene 597, respectively. The output of the dye laser was frequency-doubled in a BBO crystal for each wavelength.

The subliming molecules were detected via single-photon (VUV, 10.49 eV and 9.20 eV) ionization with a reflectron time-of-flight mass spectrometer (Jordan TOF Products, Inc.). The third harmonic of another Nd:YAG laser (ω_1=354.6 nm; Spectra Physics, Quanta Ray PRO-250-30) was frequency tripled via four-wave mixing (FWM) in a pulsed jet of xenon (Specialty Gases, 99.999%) producing pulsed (30 Hz) coherent VUV light at single-photon energy of 10.49 eV ($\omega_{VUV} = 3\omega_1$, 118.2 nm). _ENREF_52 To produce the other VUV energies (9.20 eV), resonant four-wave difference mixing was utilized ($\omega_{VUV} = 2\omega_1 - \omega_2$) by mixing ultraviolet (ω_1 = 222 nm) and visible (ω_2 = 639 nm) photons generated by Nd:YAG and dye lasers (Sirah Lasertechnik; Cobra-Stretch) using xenon as the nonlinear medium. The laser beams (ω_1, ω_2) were then focused through a UV grade fused silica window (Thorlabs; WG42012-B) and into the FWM chamber

using a fused silica bi-convex lens (Thorlabs LA4579; f = 300 mm). The generated VUV light (10.49 eV, 9.20 eV) were spatially separated from the fundamental laser beams (ω_1, ω_2) with off-axis lithium fluoride (LiF) bi-convex lens (ISP Optics, LiF-L-38-150) based on their distinct refractive indices in LiF.[3] The subliming molecules were photoionized at 1 mm above the substrate surface by VUV light and ions were extracted into the reflectron time-of-flight mass spectrometer and detected by a dual (chevron) multichannel plate (MCP) detector. The MCP signals were amplified (Ortec 9305), shaped, and recorded by a multichannel scalar (FAST ComTec, P7888-1 E) operated at 30 Hz (Quantum Composers, 9518) with a 4 ns bin width and 3600 sweeps for each mass spectrum, corresponding to one integrated mass spectrum recorded per Kelvin.

Quantum chemical calculations

CASPT2//CASSCF with an active space of 10 electrons in 9 orbitals is employed throughout the calculations. The active space includes the π and π* orbitals of acetylene and CO as well as the lone pair on the CO carbon (Figure 6 in the manuscript). CASSCF geometry optimizations employing C_{2v} symmetry employed no state averaging for the A_2 irrep. For optimizations of excited states having the B_2 irrep, no state averaging was used for the lowest triplet excited state, but 3-root equal-weight state averaging was used to optimize the second excited state since root switching occurred with the CO excited state of the same symmetry. CASPT2 calculations employed CASSCF wave functions with no state averaging for the A_1 (ground) state, 2-root equal-weight state averaging for states having A_2 symmetry, and 3-root equal-weight state averaging for states having B_2 symmetry. CASSCF geometry optimizations having C_s symmetry employed 2-root equal-weight state averaging, except for excited-state optimizations of the singlet state in the totally symmetric irrep (A′), where 3-root equal-weight state averaging was used to include the ground state and a higher excited state of the same irrep. The same state-averaging scheme is used for the CASPT2 calculations for the C_s calculations.

Table S1. Infrared absorption features of $C^{18}O$ – C_2D_2 ices before and after the UV irradiation at 5 K.

Absorptions Before Irradiation (cm^{-1})	Absorptions After Irradiation (cm^{-1})	Assignment	Carrier	References
5042		$\nu_1 + \nu_3$ (C_2D_2)	Combinations	Ref.[4]
4150		$2\nu_1$ ($C^{18}O$)	Overtone	Ref.[5]
3855		$\nu_3 + \nu_4$ (C_2H_2)	Combinations	Ref.[1]
3294		$\nu_1 + \nu_5$ (C_2D_2)	Combinations	Ref.[4]
3231		ν_3 (C_2H_2)	CH stretch	Ref.[4,6]
2929		$\nu_3 + \nu_4$ (C_2D_2)	Combination	Ref.[4]
2680		ν_1 (C_2D_2)	CD stretch	Ref.[4]
	2573	ν_4 (C_4D_4)/ ν_1 ($DC_3D^{18}O$)	CD stretch	Ref.[1,7]
2555		ν_3 (C_2HD)	CD stretch	Ref.[4]
2408		ν_3 (C_2D_2)	CD stretch	Ref.[4,8,9]
2345		ν_3 ($^{13}C_2D_2$)	CD stretch	Ref.[1]
2327		$\nu_2 + \nu_5$ (C_2D_2)	Combination	Ref.[4]
2139		ν_1 (CO)	CO stretch	Ref.[10,11]
2088		ν_1 ($C^{18}O$)	CO stretch	Ref.[11,12]
1840		ν_2 (CO)	CO stretch	Ref.[13]
	1772	ν_3 ($DC^{18}O$)	CO stretch	Ref.[1]
	1734	ν_2 (c-$C_3D_2{}^{18}O$)	CO stretch	Ref.[1]
1650		$3\nu_5$ (C_2D_2)	CO stretch	Ref.[4]
1077		$\nu_4 + \nu_5$ (C_2D_2)	Combination	Ref.[4]
706		ν_5 (C_2H_2)	CH bend	Ref.[4]
553		ν_5 (C_2D_2)	CD bend	Ref.[4]

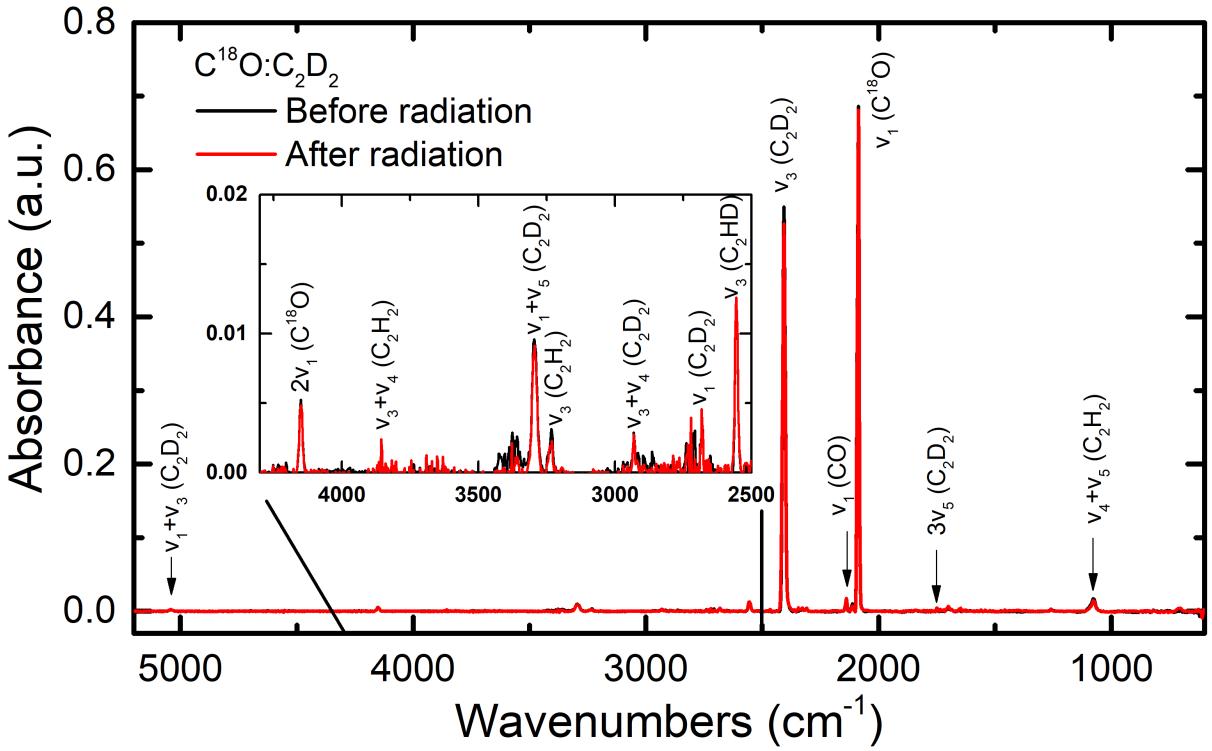

Figure S1. Infrared spectra of $C^{18}O$ – C_2D_2 ices before (black) and after (red) 222 nm irradiation for 10 hours. Their assignments are given in Table S1.

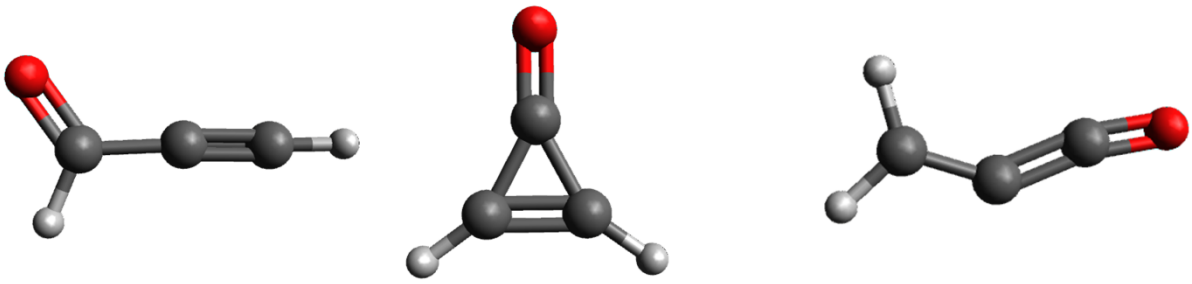

10.52 – 10.62 eV **9.22 – 9.32 eV** **9.04 – 9.14 eV**

7, Propynal **3,** Cyclopropenone **8,** Propadienone

Figure S2. Structures of the C_3H_2O isomers with their experimental ionization energies (eV),[14-16] which were corrected for the Stark effect in the experiments.[1]

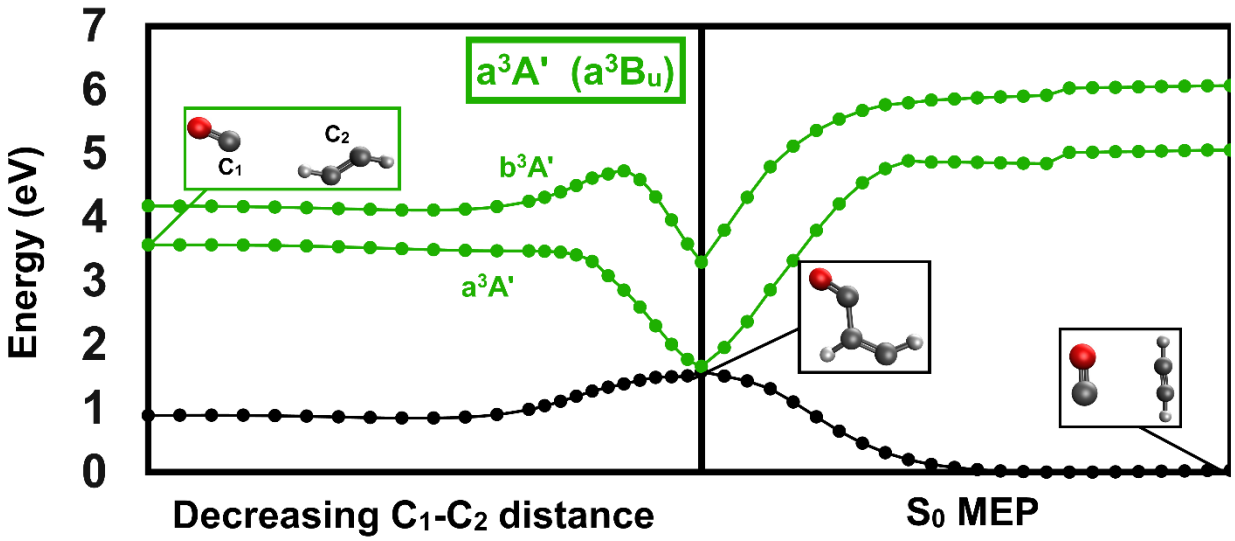

Figure S3. A combination of two calculations for the reaction of CO with the *trans* a^3B_u state of acetylene. The plot on the left is a relaxed potential energy scan for decreasing distance between the CO carbon and one of the acetylene carbons. The plot on the right is a minimum energy path (MEP) calculation on the ground state potential energy surface, starting from the a^3A' triplet state minimum geometry. The calculations were carried out without symmetry constraints, but the a^3A' triplet state minimum obtained still had C_s symmetry, indicating that the bond-formation and subsequent bond-breaking reactions follow C_s symmetry (hence the use of C_s symmetry labels, for consistency with the corresponding *cis* a^3A' calculations and labels used in the main manuscript). Triplet states are indicated in green, while singlet states are indicated in black. The lowest singlet excited state in each panel is the ground state. Energies are reported relative to the ground state equilibrium geometry of C_2H_2 and CO (i.e., with linear C_2H_2). Select structures for some points are shown in boxes. Geometry optimizations in these calculations were performed with 2-root state equal-weight state averaging CASSCF/ANO-L-VDZP, and energy calculations with CASPT2 utilizing a 5-root equal-weight state averaging CASSCF wave function.

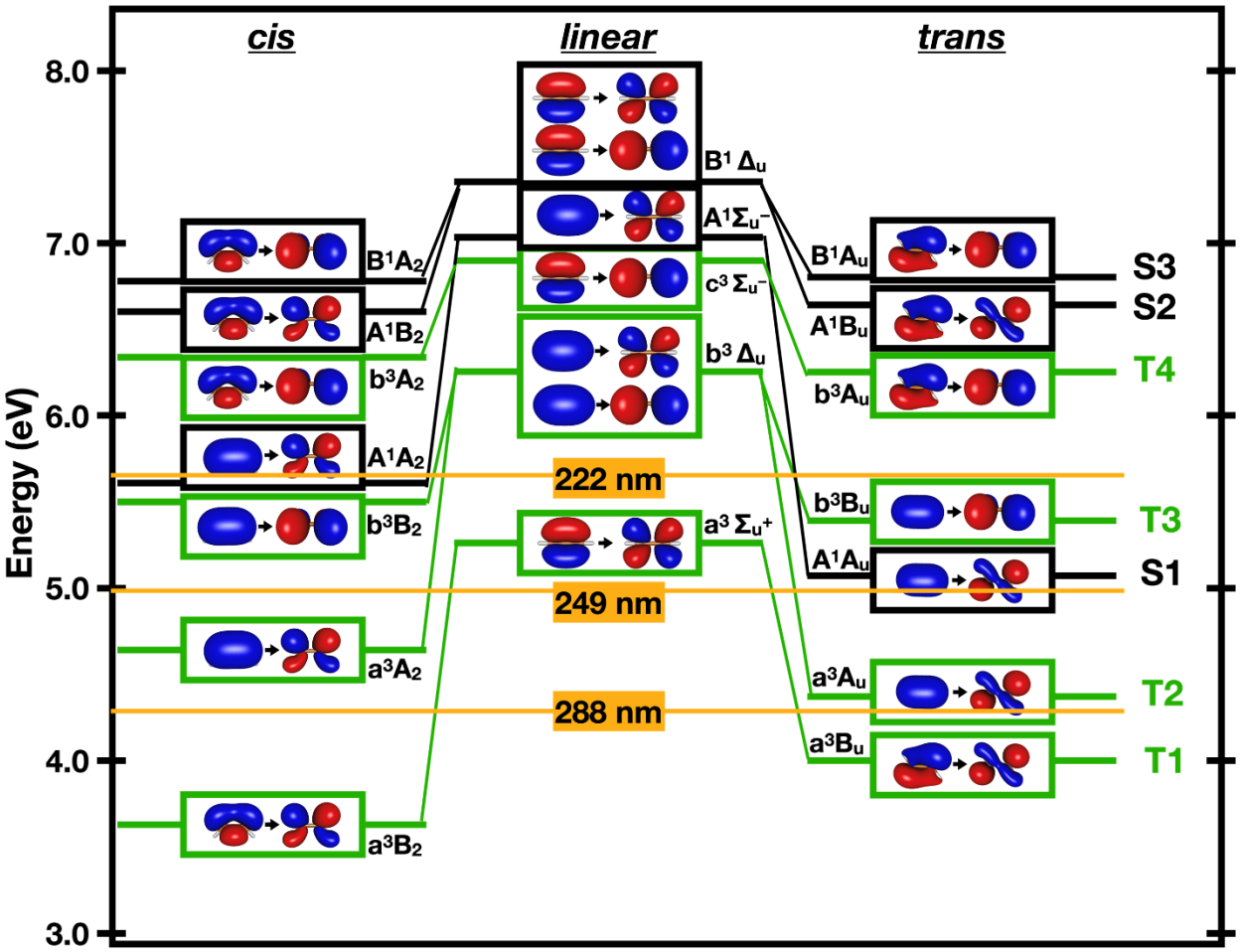

Figure S4. An overview of the low-lying triplet (green) and singlet (black) π,π* excited state energies for acetylene. Both vertical (linear geometry) and adiabatic (*cis* and *trans*) excitation energies are reported relative to the ground state equilibrium structure energy. B3LYP/6-311++G** natural transition orbitals (NTOs) are shown for each transition. For the linear excitations, the NTOs showed only represent 50% of the excitation due to symmetry. However, for the *cis* and *trans* excitations, the NTOs shown account for over 95% of the amplitude of the excitation. The energies shown are based on computed CASPT2 energies reported by Malsch et.al.[17] The excitation wavelengths employed in this work are indicated in yellow.

Cartesian coordinates of key structures, and absolute energies in atomic units.

Reference structure (separated ground state C_2H_2 and CO). S_0 Energy -190.13652380 Hartree.

C	0.00000000	0.60676924	0.19921959
C	0.00000000	-0.60676924	0.19921959
C	0.00000000	0.00000000	-4.25968511
O	0.00000000	0.00000000	-5.39108211
H	0.00000000	1.67005881	0.19529431
H	0.00000000	-1.67005881	0.19529431

c-C3H2O (cyclopropenone). S_0 Energy -190.13249548 Hartree.

C	0.0000000	-0.5568073	-1.5765856
C	0.0000000	0.7925894	-1.6022580
C	0.0000000	0.1482135	-0.3255142
O	0.0000000	0.1419567	0.8831304
H	0.0000000	-1.4463688	-2.1867966
H	0.0000000	1.6606950	-2.2427698

CASSCF-optimized ground state unstable intermediate. S_0 Energy -190.07800179 Hartree.

C	0.0000000	-0.1905200	1.9163247
C	0.0000000	0.3195795	0.6862658
C	0.0000000	-0.4044099	-0.6065987
O	0.0000000	0.1046274	-1.6961530
H	0.0000000	0.2694581	2.8923533
H	0.0000000	1.3968071	0.5779028

$\tilde{a}^3A'$ minimum structure. T_1 energy -190.07511254 Hartree.

C	0.00000000	-0.24043188	1.86494276
C	0.00000000	0.40009312	0.69034504
C	0.00000000	-0.36538390	-0.56905411
O	0.00000000	0.05802263	-1.69207127
H	0.00000000	0.09187314	2.89162818
H	0.00000000	1.48499818	0.63003540

$\tilde{b}^3A'$ minimum structure. T_2 energy -189.96298283 Hartree.

C	0.00000000	-0.31731383	1.98373074
C	0.00000000	0.37826204	0.62894237
C	0.00000000	-0.34458211	-0.60963484
O	0.00000000	0.09858276	-1.73976980
H	0.00000000	0.15371828	2.95476413
H	0.00000000	1.46050417	0.59779339

$\tilde{a}^3A''$ minimum structure. T_1 energy -190.07630947 Hartree.

C	0.00000000	-0.70726600	-2.27377239
C	0.00000000	0.42621551	-1.41086439
C	0.00000000	0.36690512	-0.05327457
O	0.00000000	0.33499022	1.10475461
H	0.00000000	-0.72958896	-3.35089165
H	0.00000000	1.43024771	-1.81512860

$\tilde{A}^1A''$ minimum structure. S_1 energy -190.04216470 Hartree.

C	0.00000000	-0.62753318	-2.28648658
C	0.00000000	0.43543695	-1.43526273
C	0.00000000	0.35742855	-0.04219274
O	0.00000000	0.31010149	1.12282939
H	0.00000000	-0.80771137	-3.34423716
H	0.00000000	1.45378117	-1.81382717

Reference

(1) Kleimeier, N. F.; Abplanalp, M. J.; Johnson, R. N.; Gozem, S.; Wandishin, J.; Shingledecker, C. N.; Kaiser, R. I. Cyclopropenone (C-C_3H_2O) as a Tracer of the Nonequilibrium Chemistry Mediated by Galactic Cosmic Rays in Interstellar Ices. *Astrophys. J.* **2021**, *911*, 24.

(2) Turner, A. M.; Abplanalp, M. J.; Chen, S. Y.; Chen, Y. T.; Chang, A. H. H.; Kaiser, R. I. A Photoionization Mass Spectroscopic Study on the Formation of Phosphanes in Low Temperature Phosphine Ices. *Phys. Chem. Chem. Phys.* **2015**, *17*, 27281-27291.

(3) VonDrasek, W. A.; Okajima, S.; Hessler, J. P. Efficient Monochromator to Isolate VUV Light Generated by Four-Wave Mixing Techniques. *Appl. Opt.* **1988**, *27*, 4057-4061.

(4) Bottger, G. L.; Jr., D. F. E. Infrared Spectra of Crystalline C_2H_2, C_2HD, and C_2D_2. *J. Chem. Phys.* **1964**, *40*, 2010-2017.

(5) Kaiser, R. I.; Maity, S.; Jones, B. M. Infrared and Reflectron Time-of-Flight Mass Spectroscopic Analysis of Methane (CH_4)–Carbon Monoxide (CO) Ices Exposed to Ionization Radiation – toward the Formation of Carbonyl-Bearing Molecules in Extraterrestrial Ices. *Phys. Chem. Chem. Phys.* **2014**, *16*, 3399-3424.

(6) Hudson, R. L.; Ferrante, R. F.; Moore, M. H. Infrared Spectra and Optical Constants of Astronomical Ices: I. Amorphous and Crystalline Acetylene. *Icarus* **2014**, *228*, 276-287.

(7) Tørneng, E.; Nielsen, C. J.; Klaeboe, P.; Hopf, H.; Priebe, H. The I.R., Raman and Microwave Spectra of 1-Butene-3-Yne (Vinylacetylene) and 1-Butene-3-Yne-4d. *Spectrochim. Acta A.* **1980**, *36*, 975-987.

(8) Abplanalp, M. J.; Kaiser, R. I. Implications for Extraterrestrial Hydrocarbon Chemistry: Analysis of Ethylene (C_2H_4) and D4-Ethylene (C_2D_4) Ices Exposed to Ionizing Radiation Via Combined Infrared Spectroscopy and Reflectron Time-of-Flight Mass Spectrometry. *Astrophys. J.* **2017**, *836*, 195.

(9) Abplanalp, M. J.; Jones, B. M.; Kaiser, R. I. Untangling the Methane Chemistry in Interstellar and Solar System Ices toward Ionizing Radiation: A Combined Infrared and Reflectron Time-of-Flight Analysis. *Phys. Chem. Chem. Phys.* **2018**, *20*, 5435-5468.

(10) Cuylle, S. H.; Zhao, D.; Strazzulla, G.; Linnartz, H. Vacuum Ultraviolet Photochemistry of Solid Acetylene: A Multispectral Approach. *A&A* **2014**, *570*, A83.

(11) Bennett, C. J.; Jamieson, C.; Mebel, A. M.; Kaiser, R. I. Untangling the Formation of the Cyclic Carbon Trioxide Isomer in Low Temperature Carbon Dioxide Ices. *Phys. Chem. Chem. Phys.* **2004**, *6*, 735-746.

(12) Jamieson, C. S.; Mebel, A. M.; Kaiser, R. I. Understanding the Kinetics and Dynamics of Radiation-Induced Reaction Pathways in Carbon Monoxide Ice at 10 K. *Astrophys. J., Suppl. Ser.* **2006**, *163*, 184-206.

(13) Zhou, L.; Kaiser, R. I.; Gao, L. G.; Chang, A. H. H.; Liang, M. C.; Yung, Y. L. Pathways to Oxygen-Bearing Molecules in the Interstellar Medium and in Planetary Atmospheres: Cyclopropenone (C-C_3H_2O) and Propynal (HCCCHO). *Astrophys. J.* **2008**, *686*, 1493-1502.

(14) von Niessen, W.; Bieri, G.; Åsbrink, L. 30.4-Nm He (II) Photoelectron Spectra of Organic Molecules: Part III. Oxo-Compounds (C, H, O). *J. Electron Spectrosc. Relat. Phenom.* **1980**, *21*, 175-191.

(15) Harshbarger, W. R.; Kuebler, N. A.; Robin, M. B. Electronic Structure and Spectra of Small Rings. V Photoelectron and Electron Impact Spectra of Cyclopropenone. *J. Chem. Phys.* **1974**, *60*, 345-350.

(16) Terlouw, J. K.; Holmes, J. L.; Lossing, F. P. Ionized Ethylidene Ketene and Its Homologue Methylene Ketene. *Can. J. Chem.* **1983**, *61*, 1722-1724.

(17) Malsch, K.; Rebentisch, R.; Swiderek, P.; Hohlneicher, G. Excited States of Acetylene: A CASPT2 Study. *Theor. Chem. Acc.* **1998**, *100*, 171-182.